



**HAL**  
open science

# Robust output regulation of 2 2 hyperbolic systems part I: Control law and Input-to-State Stability

Pierre-Olivier Lamare, Jean Auriol, Ulf Jakob F Aarsnes, Florent Di Meglio

## ► To cite this version:

Pierre-Olivier Lamare, Jean Auriol, Ulf Jakob F Aarsnes, Florent Di Meglio. Robust output regulation of 2 2 hyperbolic systems part I: Control law and Input-to-State Stability. 2017. hal-01499686v1

**HAL Id: hal-01499686**

**<https://hal.science/hal-01499686v1>**

Preprint submitted on 31 Mar 2017 (v1), last revised 16 Oct 2017 (v2)

**HAL** is a multi-disciplinary open access archive for the deposit and dissemination of scientific research documents, whether they are published or not. The documents may come from teaching and research institutions in France or abroad, or from public or private research centers.

L'archive ouverte pluridisciplinaire **HAL**, est destinée au dépôt et à la diffusion de documents scientifiques de niveau recherche, publiés ou non, émanant des établissements d'enseignement et de recherche français ou étrangers, des laboratoires publics ou privés.

# Performance trade-offs in the observer design of a $2 \times 2$ linear hyperbolic system

Jean Auriol<sup>1</sup>, Ulf Jakob F. Aarsnes<sup>2</sup> and Florent Di Meglio<sup>3</sup>

**Abstract**—In this paper, we introduce a degree of freedom in the design of backstepping observers for linear hyperbolic systems. This enables tuning of observer and controller feedback aggressiveness, through a trade-off between performance and noise sensitivity. This constitutes an important step towards practical implementation of such observers, notably in observer-controller schemes. The results are illustrated by frequency analysis of the gang of four and time-domain simulations.

## I. INTRODUCTION

This article presents an extension to the collocated boundary observer presented in [17], for a system of two heterodirectional first-order hyperbolic linear PDEs, in presence of disturbances in the system and of noise in the measurements. In particular, the observer designed in this article presents a degree of freedom that can increase sensitivity-performance.

Most physical systems involving a transport phenomenon can be modeled using hyperbolic partial differential equations (PDEs): traffic flow [1], heat exchangers [19], open channel flow [5], [8] or multiphase flow [9], [10]. The backstepping approach [11], [15] has enabled the design of stabilizing full-state feedback laws for these systems. These controllers are *explicit*, in the sense that they are expressed as a linear functional of the distributed state at each instant. The (distributed) gains can be computed offline. The generalization of these stabilization results for a large number of equations has been done during the last few years ([3], [6], [11]). However, to enable application of these backstepping results to industrial control-problems, the issues of noise sensitivity, robustness and performance trade-offs have to be better addressed. As an example, the backstepping results typically yield a single controller for a given system without any tuning capability.

The main contribution of this paper is a tunable observer for linear hyperbolic systems. Using the backstepping approach, an extension to the observer presented in [17] in presence of disturbances in the system and of noise in the measurements is derived. This new observer provides an additional degree of freedom which enables performance trade-offs in the design between actuation noise sensitivity and

convergence rate. Our approach to analyze the performance of this new observer is the following: using the Laplace transform we derive the systems loop transfer function [7], from which the load sensitivity and noise sensitivity functions can be found [2], [20] which illustrate the trade-off represented by the new degree of freedom in the design.

The paper is organized as follows. In Section II-A, we introduce the model equations and the notations; in particular we introduce noise and disturbances in the ideal model. The output feedback controller designed in [17] to stabilize the ideal model in finite time is presented in Section II-B. Retaining the backstepping approach, the new observer, that provides an additional degree of freedom, is presented in Section III. The transfer function of the closed-loop system is computed in Section IV which enables the derivation of the gang of four sensitivity functions. Finally, the result and trade-off is illustrated by an example in Section V.

## II. PROBLEM DESCRIPTION

### A. System under consideration

We consider the following 2-state linear hyperbolic system

$$u_t(t, x) + \lambda u_x(t, x) = \sigma^{+-} v(t, x) \quad (1)$$

$$v_t(t, x) - \mu v_x(t, x) = \sigma^{-+} u(t, x) \quad (2)$$

evolving in  $\{(t, x) \mid t > 0, x \in [0, 1]\}$ , with the following linear boundary conditions

$$u(t, 0) = qv(t, 0) + d_1(t), \quad (3)$$

$$v(t, 1) = \rho u(t, 1) + d_2(t) + U(t) \quad (4)$$

with constant inside-domain coupling terms and constant speeds  $\lambda$  and  $\mu$ . The boundary couplings  $q$  and  $\rho$  are assumed non-null. The initial conditions denoted  $u_0$  and  $v_0$  are assumed to belong to  $L^2([0, 1])$ . The terms  $d_1(t)$  and  $d_2(t)$  represent unknown disturbances acting on the boundaries. The sensor is located at the right boundary, i.e we measure

$$y(t) = u(t, 1) + n(t) \quad (5)$$

where  $n(t)$  represents an unknown noise term. The variable  $U(t)$  represents the control input. The system is schematically depicted on Figure 1.

*Remark 1:* The scalar coupling terms  $\sigma^{+-}$  and  $\sigma^{-+}$  are assumed constant here but the results of this paper can be adjusted for spatially-varying coupling terms or and velocities.

<sup>1</sup>Jean Auriol is with MINES ParisTech, PSL Research University, CAS - Centre automatique et systèmes, 60 bd St Michel 75006 Paris, France. jean.auriol@mines-paristech.fr

<sup>2</sup>Ulf Jakob F. Aarsnes is International Research Institute of Stavanger (IRIS), Oslo, Norway and DrillWell - Drilling and well centre for improved recovery, Stavanger, Norway ujfa@iris.no

<sup>3</sup>Florent Di Meglio is with MINES ParisTech, PSL Research University, CAS - Centre automatique et systèmes, 60 bd St Michel 75006 Paris, France. florent.di.meglio@mines-paristech.fr

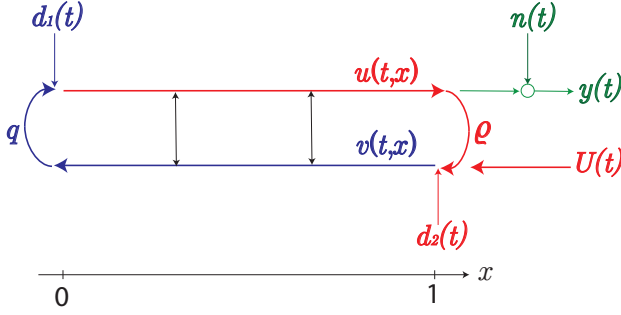


Fig. 1. Schematic representation of system (1)-(5)

*Remark 2:* The system formulation (1)-(2) encompasses systems on the form

$$u_t(t, x) + \lambda u_x(t, x) = \sigma^{++} u(t, x) + \sigma^{+-} v(t, x) \quad (6)$$

$$v_t(t, x) - \mu v_x(t, x) = \sigma^{-+} u(t, x) + \sigma^{--} v(t, x) \quad (7)$$

through a variable change as presented in [16].

### B. Output feedback controller in the ideal case

In the absence of disturbance or noise (i.e.  $d_1(t) = d_2(t) = n(t) = 0$ ), a collocated output feedback controller has been derived in [18, Theorem 3]: there exist kernels  $P^{uu}, P^{uv}, P^{vu}, P^{vv}, K^{vu}$  and  $K^{vv}$  defined on  $\mathcal{T} = \{(x, \xi) \in [0, 1]^2 | x \leq \xi\}$  such that the following theorem holds:

*Theorem 1:* [18] Consider system (1)-(4) with initial conditions  $u_0$  and  $v_0$ , with  $d_1(t) = d_2(t) = n(t) = 0$  and with control law

$$U = -\rho \hat{u}(t, 1) + \int_0^1 K^{vu}(1, \xi) \hat{u}(\xi, t) + K^{vv}(1, \xi) \hat{v}(\xi, t) d\xi \quad (8)$$

where  $\hat{u}$  and  $\hat{v}$  are computed from

$$\hat{u}_t = -\lambda \hat{u}_x + \sigma^{+-} \hat{v} - \lambda P^{uu}(u(t, 1) - \hat{u}(t, 1)) \quad (9)$$

$$\hat{v}_t = \mu \hat{v}_x + \sigma^{-+} \hat{u} - \lambda P^{vv}(v(t, 1) - \hat{v}(t, 1)) \quad (10)$$

$$\hat{u}(t, 0) = q \hat{v}(t, 0), \quad \hat{v}(t, 1) = \rho u(t, 1) + U(t) \quad (11)$$

Its null-equilibrium is exponentially stable and is reached in finite time  $t = 2(\frac{1}{\lambda} + \frac{1}{\mu})$ .

### C. Formulation of the problem

The controller used in Theorem 1 stirs the system to zero in finite time but does not take into account the closed loop performance with regards to noise or disturbances, which is of significant importance in practical application. The first goal of this article is to derive a new observer with an additional *degree of freedom* which enables performance trade-offs in the design, e.g. between actuation noise sensitivity and convergence rate. This is the topic of the next section.

## III. COLLOCATED OBSERVER DESIGN

In this section we design an observer that relies on the noisy measurements at the right boundary:  $y(t) = u(t, 1) + n(t)$ . This observer will be designed as a function of a parameter  $\epsilon$  that represents a trade-off between measurement reliability versus that of the model. The uncertainty of the measurement and the model is represented by the noise and the disturbances, respectively.

### A. Observer design

Similarly to [18], the observer equations read as follows

$$\hat{u}_t(t, x) + \lambda \hat{u}_x(t, x) = \sigma^{+-} \hat{v}(t, x) - P^+(x)(\hat{u}(t, 1) - y(t)) \quad (12)$$

$$\hat{v}_t(t, x) - \mu \hat{v}_x(t, x) = \sigma^{-+} \hat{u}(t, x) - P^-(x)(\hat{u}(t, 1) - y(t)) \quad (13)$$

with the modified boundary conditions

$$\hat{u}(t, 0) = q \hat{v}(t, 0), \quad (14)$$

$$\hat{v}(t, 1) = \rho(1 - \epsilon) \hat{u}(t, 1) + \rho \epsilon y(t) + U(t) \quad (15)$$

where  $P^+(\cdot)$  and  $P^-(\cdot)$  are defined as

$$P^+(x) = -\lambda P^{uu}(x, 1) + \mu \rho(1 - \epsilon) P^{uv}(x, 1) \quad (16)$$

$$P^-(x) = -\lambda P^{vu}(x, 1) + \mu \rho(1 - \epsilon) P^{vv}(x, 1) \quad (17)$$

where the kernels  $P^{uu}, P^{uv}, P^{vu}$  and  $P^{vv}$  are defined in [18].

*Remark 3:* The coefficient  $\epsilon \in [0, 1]$  in (15) can be interpreted as a measure of trust in our measurements relative to the model (or unmeasured disturbances), where  $\epsilon = 1$  results in relying more on the measurements and  $\epsilon = 0$  relying more on the model. This trade-off will be made explicit in the magnitude of  $d_1$  and  $d_2$  relative to  $n$  in the following.

*Remark 4:* The coefficient  $\epsilon$  cannot be chosen arbitrarily in  $[0, 1]$ . As it will appear in the next subsection, it has to be close enough to 1 to ensure the convergence of the observer.

Applying the observer (12)–(15) to the system (1)–(4) yields the error system (denoting  $\tilde{u}(t, x) = u(t, x) - \hat{u}(t, x)$  and  $\tilde{v}(t, x) = v(t, x) - \hat{v}(t, x)$ ):

$$\tilde{u}_t(t, x) + \lambda \tilde{u}_x(t, x) = \sigma^{+-} \tilde{v}(t, x) - P^+(x) \tilde{u}(t, 1) - n(t) P^+(x) \quad (18)$$

$$\tilde{v}_t(t, x) - \mu \tilde{v}_x(t, x) = \sigma^{-+} \tilde{u}(t, x) - P^-(x) \tilde{u}(t, 1) - n(t) P^-(x) \quad (19)$$

with the boundary conditions

$$\tilde{u}(t, 0) = q \tilde{v}(t, 0) + d_1(t), \quad (20)$$

$$\tilde{v}(t, 1) = d_2(t) + \rho(1 - \epsilon) \tilde{u}(t, 1) - \rho \epsilon n(t) \quad (21)$$

### B. Ideal error system

In this section, we consider the unperturbed system with uncorrupted measurements; to give insight on the impact of  $\epsilon$  in the ideal case. Using the backstepping approach and a Volterra transformation identical to the one presented in

[18], we can map system (18)-(21) to a simpler target system. Consider the kernels  $P^{uu}$ ,  $P^{uv}$ ,  $P^{vu}$  and  $P^{vv}$  defined in [18] and the following Volterra transformation

$$\tilde{u}(t, x) = \tilde{\alpha}_{id}(t, x) - \int_x^1 (P^{uu}(x, \xi)\tilde{\alpha}_{id}(t, \xi) + P^{uv}(x, \xi)\tilde{\beta}_{id}(t, \xi))d\xi \quad (22)$$

$$\tilde{v}(t, x) = \tilde{\beta}_{id}(t, x) - \int_x^1 (P^{vu}(x, \xi)\tilde{\alpha}_{id}(t, \xi) + P^{vv}(x, \xi)\tilde{\beta}_{id}(t, \xi))d\xi \quad (23)$$

Differentiating (22) and (23) with respect to space and time, one can easily prove that system (18)-(21) is equivalent to the following system

$$(\tilde{\alpha}_{id})_t(t, x) + \lambda(\tilde{\alpha}_{id})_x(t, x) = 0 \quad (24)$$

$$(\tilde{\beta}_{id})_t(t, x) - \mu(\tilde{\beta}_{id})_x(t, x) = 0 \quad (25)$$

with the following boundary conditions

$$\tilde{\alpha}_{id}(t, 0) = q\tilde{\beta}_{id}(t, 0) \quad (26)$$

$$\tilde{\beta}_{id}(t, 1) = \rho(1 - \epsilon)\tilde{\alpha}_{id}(t, 1) \quad (27)$$

We then have the following lemma

*Lemma 1:* System (24)-(27) is exponentially stable if and only if

$$1 - \frac{1}{|\rho q|} < \epsilon \leq 1 \quad (28)$$

*Remark 5:* In the case  $\epsilon = 1$  we have the same target system as the one presented in [18]. It converges in finite time  $\frac{1}{\lambda} + \frac{1}{\mu}$  to zero.

### C. Error system including noise and disturbance

We consider in this section the real error-system (18)-(21), including the noise and disturbances  $n, d_1, d_2$ . Applying the Volterra transformation (22)-(23), system (18)-(21) can be mapped to the following target system

$$\tilde{\alpha}_t(t, x) + \lambda\tilde{\alpha}_x(t, x) = n(t)f_1(x) + d_2(t)f_2(x) \quad (29)$$

$$\tilde{\beta}_t(t, x) - \mu\tilde{\beta}_x(t, x) = n(t)f_3(x) + d_2(t)f_4(x) \quad (30)$$

with the boundary conditions

$$\tilde{\alpha}(t, 0) = q\tilde{\beta}(t, 0) + d_1(t) \quad (31)$$

$$\tilde{\beta}(t, 1) = d_2(t) + \rho(1 - \epsilon)\tilde{\alpha}(t, 1) - \rho\epsilon n(t) \quad (32)$$

where  $f_1, f_2, f_3$  and  $f_4$  are the solutions of the following integral equations

$$f_1(x) = -P^+(x) - \mu\rho\epsilon P^{uv}(x, 1) - \int_x^1 P^{uu}(x, \xi)f_1(\xi) + P^{uv}(x, \xi)f_3(\xi)d\xi \quad (33)$$

$$f_2(x) = \mu P^{uv}(x, 1) + \int_x^1 P^{uu}(x, \xi)f_2(\xi) + P^{uv}(x, \xi)f_4(\xi)d\xi \quad (34)$$

$$f_3(x) = -P^-(x) - \mu\rho\epsilon P^{vv}(x, 1) - \int_x^1 P^{vv}(x, \xi)f_3(\xi) + P^{vu}(x, \xi)f_1(\xi)d\xi \quad (35)$$

$$f_4(x) = \mu P^{vv}(x, 1) + \int_x^1 P^{vv}(x, \xi)f_4(\xi) + P^{vu}(x, \xi)f_2(\xi)d\xi \quad (36)$$

One can prove that this system is Input-State-Stable (ISS) with respect to  $d_1, d_2$  and  $n$  and remains consequently stable in presence of noise and disturbances.

*Proof: (Sketch)* Assume that  $n(t) = d_1(t) = 0$ , consider the following Lyapunov function

$$V(t) = \int_0^1 \frac{p}{\lambda} e^{-\delta x} \tilde{\alpha}^2(t, x) + \frac{l}{\mu} e^{\delta x} \tilde{\beta}^2(t, x) dx \quad (37)$$

where  $p, l$  and  $\delta$  are positive constant such that

$$pq^2 < l \quad l e^{2\delta} (\rho(1 - \epsilon))^2 < p \quad (38)$$

With these conditions, differentiating  $V$  and using Young's inequalities yields

$$\dot{V}(t) \leq - \int_0^1 [(\delta p e^{-\delta x} - \frac{1}{K^2}) \tilde{\alpha}^2(t, x) + (\delta l e^{\delta x} - \frac{1}{K^2}) \tilde{\beta}^2(t, x)] dx + d_2^2(t)g(K^2) \quad (39)$$

where  $K$  can be chosen as large as necessary and with  $g$  a positive function of  $K^2$ . Taking  $K$  large enough yields the expected result. ■

## IV. FREQUENCY DOMAIN ANALYSIS

In order to analyze the performance of the output-feedback controller (8), (12)-(17) in presence of noise and disturbances, we derive in the next section the closed loop transfer function of system (29)-(32), with inputs  $n, d_1, d_2$  and outputs  $y$  and  $U$ . To obtain these transfer functions we divide the system in three subsystems

- The controlled system whose direct inputs are  $d_1, d_2$  and  $U(t)$  and whose direct output is  $u(t, 1)$
- The observer whose direct inputs are  $y(t)$  and  $U(t)$  and whose outputs are  $\hat{u}$  and  $\hat{v}$ .
- The controller whose direct inputs are  $\hat{u}$  and  $\hat{v}$  and whose output is  $U(t)$

We denote  $s$  the Laplace variable. The Laplace transform of  $u(t, x)$  will be denoted  $\mathbf{u}(s, x)$ . Moreover, we denote in the following  $\hat{w}(t, x) = (\hat{u}(t, x), \hat{v}(t, x))^T$ .

The feedback system satisfies the canonical block diagram shown in Figure 2, with the transfer functions

$$\frac{\mathbf{y}}{\mathbf{U}}(s) = \mathbf{P}(s), \quad \frac{\mathbf{U}}{\mathbf{y}}(s) = \mathbf{C}(s). \quad (40)$$

### A. Computation of the Gang of Four

The four transfer functions mapping  $n, d_2$  to  $y, U(s)$  form the canonical *Gang of Four* [2], the evaluation of which are considered essential for the practical implementation of any feedback control system. They are defined as

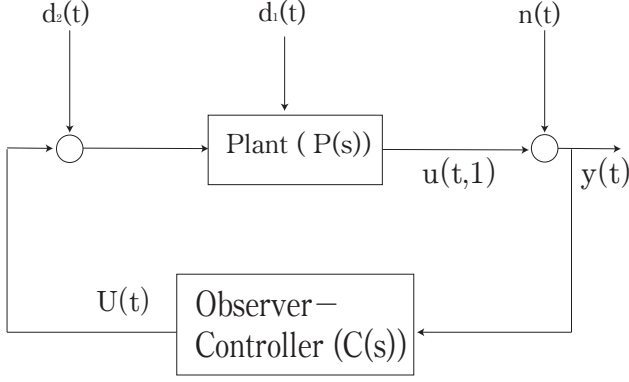


Fig. 2. Block representation of the closed-loop system

- Load sensitivity function

$$\mathbf{P}\mathbf{S}(s) = \frac{\mathbf{y}}{\mathbf{d}_2}(s) = \frac{\mathbf{P}(s)}{1 + \mathbf{P}(s)\mathbf{C}(s)} \quad (41)$$

- Sensitivity function

$$\mathbf{S}(s) = \frac{\mathbf{y}}{\mathbf{n}}(s) = \frac{-1}{1 + \mathbf{P}(s)\mathbf{C}(s)} \quad (42)$$

- Complementary sensitivity function

$$\mathbf{T}(s) = \frac{\mathbf{U}}{\mathbf{d}_2}(s) = -\frac{\mathbf{P}(s)\mathbf{C}(s)}{1 + \mathbf{P}(s)\mathbf{C}(s)} \quad (43)$$

- Noise sensitivity function

$$\mathbf{C}\mathbf{S}(s) = \frac{\mathbf{U}}{\mathbf{n}}(s) = \frac{\mathbf{C}(s)}{1 + \mathbf{P}(s)\mathbf{C}(s)} \quad (44)$$

In the next section we derive the transfer functions  $\mathbf{C}(s)$  and  $\mathbf{P}(s)$ .

### B. Transfer function of the controlled system

We consider in this subsection the subsystem composed of equations (1)-(4). The objective is to obtain a relation between  $\mathbf{y}(s)$ ,  $\mathbf{U}(s)$ ,  $\mathbf{d}_1(s)$  and  $\mathbf{d}_2(s)$ . Taking the Laplace transform of the subsystem (1)-(2) yields

$$\frac{d}{dx} \begin{pmatrix} \mathbf{u}(s, x) \\ \mathbf{v}(s, x) \end{pmatrix} = \begin{pmatrix} -\frac{s}{\lambda} & \frac{\sigma^{+-}}{\lambda} \\ -\frac{\sigma^{-+}}{\mu} & \frac{s}{\mu} \end{pmatrix} \begin{pmatrix} \mathbf{u}(s, x) \\ \mathbf{v}(s, x) \end{pmatrix} \quad (45)$$

In the following we denote

$$\mathbf{A}(s) = \begin{pmatrix} -\frac{s}{\lambda} & \frac{\sigma^{+-}}{\lambda} \\ -\frac{\sigma^{-+}}{\mu} & \frac{s}{\mu} \end{pmatrix} \quad (46)$$

$$\mathbf{B}(s, x) = \begin{pmatrix} \mathbf{b}_{11}(s, x) & \mathbf{b}_{12}(s, x) \\ \mathbf{b}_{21}(s, x) & \mathbf{b}_{22}(s, x) \end{pmatrix} = \exp(\mathbf{A}(s)x) \quad (47)$$

It yields

$$\mathbf{u}(s, x) = \mathbf{b}_{11}(s, x)\mathbf{u}(s, 0) + \mathbf{b}_{12}(s, x)\mathbf{v}(s, 0) \quad (48)$$

$$\mathbf{v}(s, x) = \mathbf{b}_{21}(s, x)\mathbf{u}(s, 0) + \mathbf{b}_{22}(s, x)\mathbf{v}(s, 0) \quad (49)$$

Rewriting the boundary conditions (3)-(4) yields:

$$\mathbf{u}(s, 0) = q\mathbf{v}(s, 0) + \mathbf{d}_1(s) \quad (50)$$

$$\mathbf{v}(s, 1) = \rho\mathbf{b}(s, 1) + \mathbf{d}_2(s) + \mathbf{U}(s) \quad (51)$$

Consequently, we obtain after some computation

$$\mathbf{u}(s, 1) = \mathbf{H}(s)\mathbf{d}_1(s) + \mathbf{P}(s)\mathbf{d}_2(s) + \mathbf{P}(s)\mathbf{U}(s) \quad (52)$$

where  $\mathbf{H}(s)$  and  $\mathbf{P}(s)$  are defined by

$$\mathbf{H}(s) = \frac{(\mathbf{b}_{11}(s, 1) - \mathbf{b}_{21}(s, 1)\mathbf{H}_0(s))}{1 - \rho\mathbf{H}_0(s)} \quad (53)$$

$$\mathbf{P}(s) = \frac{\mathbf{H}_0(s)}{1 - \rho\mathbf{H}_0(s)} \quad (54)$$

$$\text{with } \mathbf{H}_0(s) = \frac{q\mathbf{b}_{11}(s, 1) + \mathbf{b}_{12}(s, 1)}{q\mathbf{b}_{21}(s, 1) + \mathbf{b}_{22}(s, 1)} \quad (55)$$

It immediately yields

$$\mathbf{y}(s) = \mathbf{H}(s)\mathbf{d}_1(s) + \mathbf{P}(s)\mathbf{d}_2(s) + \mathbf{P}(s)\mathbf{U}(s) - \mathbf{n}(s) \quad (56)$$

$\mathbf{P}(s)$  represents the plant block.

### C. Transfer function of the observer

We consider in this subsection the subsystem (18)-(21). We compute the transfer function between  $\hat{w}(t, x)$  and  $y(t)$  and the transfer function between  $\hat{w}(t, x)$  and  $U(t)$ .

Taking the Laplace transform of (18)-(19) yields

$$\frac{d}{dx} \hat{\mathbf{w}}(s, x) = \begin{pmatrix} \lambda & 0 \\ 0 & -\mu \end{pmatrix}^{-1} \left[ \begin{pmatrix} -s & \sigma^{+-} \\ \sigma^{-+} & -s \end{pmatrix} \hat{\mathbf{w}} - \begin{pmatrix} P^+(x) \\ P^-(x) \end{pmatrix} (\hat{\mathbf{u}}(s, 1) - \mathbf{y}(s)) \right] \quad (57)$$

Since the boundary term  $\hat{\mathbf{u}}(x, 1)$  is inside the equation we have to solve this equation in retrograde space. We consequently denote

$$\hat{\underline{\mathbf{w}}}(s, x) = \hat{\mathbf{w}}(s, 1 - x), \quad \hat{\underline{\mathbf{u}}}(s, 0) = \hat{\mathbf{u}}(s, 0) \quad (58)$$

$$\underline{\underline{\Lambda}} = \begin{pmatrix} -\lambda & 0 \\ 0 & \mu \end{pmatrix}, \quad \underline{\underline{\Sigma}} = \begin{pmatrix} 0 & \sigma^{+-} \\ \sigma^{-+} & 0 \end{pmatrix} \quad (59)$$

$$\underline{\underline{\mathbf{D}}}(s) = \underline{\underline{\Lambda}}^{-1}(\underline{\underline{\Sigma}} - sI_2), \quad \underline{\underline{\mathbf{P}}}(x) = \begin{pmatrix} P^+(1-x) \\ P^-(1-x) \end{pmatrix} \quad (60)$$

Consequently (57) can be rewritten as

$$\frac{d}{dx} \hat{\underline{\mathbf{w}}}(s, x) = \underline{\underline{\mathbf{D}}}(s)\hat{\underline{\mathbf{w}}} - \underline{\underline{\Lambda}}^{-1}[\underline{\underline{\mathbf{P}}}(x)(\hat{\underline{\mathbf{u}}}(s, 0) - \mathbf{y}(s))] \quad (61)$$

The ODE (61) is well-posed and can be implicitly solved. The general structure of the solutions is given by

$$\hat{\underline{\mathbf{w}}}(s, x) = \underline{\underline{\Phi}}_w(x, s)\hat{\underline{\mathbf{w}}}(s, 0) + \underline{\underline{\Phi}}_y(x, s)\mathbf{y}(s) \quad (62)$$

where  $\underline{\underline{\Phi}}_w(x)$  and  $\underline{\underline{\Phi}}_y(x) \in \mathcal{M}^{2,2} \times \mathcal{M}^{2,1}$ . We denote  $(\underline{\underline{\Phi}}_w)_1$  (resp.  $(\underline{\underline{\Phi}}_w)_2$ ) the first (resp. second) column of  $\underline{\underline{\Phi}}_w$ . Their expressions are obtained solving (61) with  $y = 0$  and the initial condition  $\hat{\underline{\mathbf{w}}}(s, 0) = \begin{pmatrix} 1 \\ 0 \end{pmatrix}$  (resp.  $\begin{pmatrix} 0 \\ 1 \end{pmatrix}$ ). It yields

$$\begin{aligned} (\underline{\underline{\Phi}}_w)_1(x, s) &= \exp(\underline{\underline{\mathbf{D}}}(s)x) \begin{pmatrix} 1 & 0 \end{pmatrix}^T \\ &\quad - \int_0^x \exp((x-\nu)\underline{\underline{\mathbf{D}}}(s)) \underline{\underline{\Lambda}}^{-1} \underline{\underline{\mathbf{P}}}(\nu) d\nu \end{aligned} \quad (63)$$

$$(\underline{\underline{\Phi}}_w)_2(x, s) = \exp(\underline{\underline{\mathbf{D}}}(s)x) \begin{pmatrix} 0 & 1 \end{pmatrix}^T \quad (64)$$

Similarly, solving (61) with  $y = 1$  and the initial condition  $\hat{\mathbf{w}}(s, 0) = 0$  yields the expression of  $\Phi_y$

$$\Phi_y(x, s) = \int_0^x \exp((x - \nu)\mathbf{D}(s))\underline{\Delta}^{-1}\underline{P}(\nu)d\nu \quad (65)$$

Consequently, we have

$$\hat{\mathbf{w}}(s, x) = \Phi_w(1 - x, s)\hat{\mathbf{w}}(s, 1) + \Phi_y(1 - x, s)\mathbf{y}(s) \quad (66)$$

We now use the boundary conditions (14)-(15) We have

$$(-\rho(1 - \epsilon) \quad 1) \hat{\mathbf{w}}(s, 1) = \rho\epsilon\mathbf{y}(s) + \mathbf{U}(s) \quad (67)$$

$$(1 \quad -q)\hat{\mathbf{w}}(s, 0) = 0 \quad (68)$$

We have

$$\hat{\mathbf{w}}(s, 0) = \Phi_w(1, s)\hat{\mathbf{w}}(s, 1) + \Phi_y(1, s)\mathbf{y}(s) \quad (69)$$

Denoting  $\mathbf{K}(s) = \begin{pmatrix} -(1 - q)\Phi_w(1, s) \\ -\rho(1 - \epsilon) & 1 \end{pmatrix}$ , it yields

$$\mathbf{K}(s)\hat{\mathbf{w}}(s, 1) = \begin{pmatrix} 0 \\ 1 \end{pmatrix} \mathbf{U}(s) + \begin{pmatrix} (1 - q)\Phi_y(1, s) \\ \rho\epsilon \end{pmatrix} \mathbf{y}(s) \quad (70)$$

Consequently, one has

$$\begin{aligned} \hat{\mathbf{w}}(s, x) &= \Phi_w(1 - x, s)\mathbf{K}(s)^{-1} \begin{pmatrix} 0 \\ 1 \end{pmatrix} \mathbf{U}(s) \\ &+ (\Phi_w(1 - x, s)\mathbf{K}(s)^{-1} \begin{pmatrix} (1 - q)\Phi_y(1, s) \\ \rho\epsilon \end{pmatrix}) \\ &+ \Phi_y(1 - x, s)\mathbf{y}(s) \end{aligned} \quad (71)$$

Thus,

$$\hat{\mathbf{w}}(s, x) = \mathbf{H}_U(s, x)\mathbf{U}(s) + \mathbf{H}_y(s, x)\mathbf{y}(s) \quad (72)$$

#### D. Transfer function of the control law

We consider in this section the control law (8). We now compute (using (72)) a relation between  $\mathbf{y}(s)$  and  $\mathbf{U}(s)$ . In the following, we denote

$$R = (\rho \quad 0), \quad M(\xi) = (K(1, \xi) \quad L(1, \xi)) \quad (73)$$

We immediately have from (8)

$$\mathbf{U}(s) = -R\hat{\mathbf{w}}(s, 1) + \int_0^1 M(\xi)\hat{\mathbf{w}}(s, \xi)d\xi \quad (74)$$

Using (72) yields

$$\begin{aligned} \mathbf{U}(s) &= -R(\mathbf{H}_U(s, 1)\mathbf{U}(s) + \mathbf{H}_y(s, 1)\mathbf{y}(s)) \\ &+ \left( \int_0^1 M(\xi)\mathbf{H}_U(s, \xi)d\xi \right) \mathbf{U}(s) \\ &+ \left( \int_0^1 M(\xi)\mathbf{H}_y(s, \xi)d\xi \right) \mathbf{y}(s) \end{aligned} \quad (75)$$

and consequently

$$\mathbf{U}(s) = -\mathbf{C}(s)\mathbf{y}(s) \quad (76)$$

where

$$\mathbf{C}(s) = \frac{R\mathbf{H}_y(s, 1) - \int_0^1 M(\xi)\mathbf{H}_y(s, \xi)d\xi}{1 + R\mathbf{H}_U(1, s) - \int_0^1 M(\xi)\mathbf{H}_U(s, \xi)d\xi} \quad (77)$$

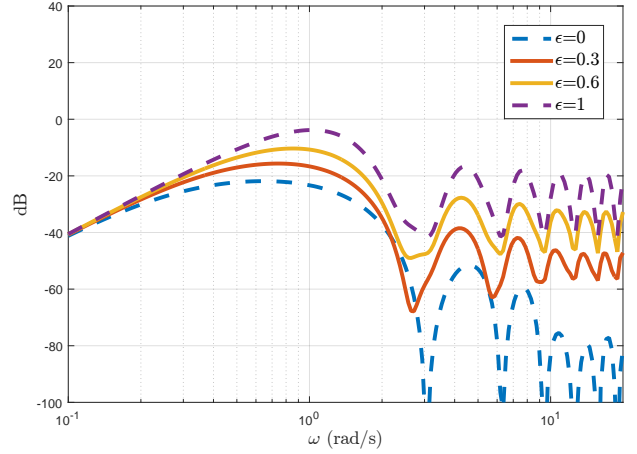


Fig. 3. Noise sensitivity function, CS, for different values of  $\epsilon$

$\mathbf{C}(s)$  represents the feedback block (including the observer). Using these expressions it is henceforth possible to compute numerically the transfer functions of the Gang of Four. In the following section these transfer functions are analyzed for a particular example.

*Remark 6:* In order to fulfill the closed loop analysis one could compute the two last transfer functions between  $\mathbf{y}(s)$  and  $\mathbf{d}_1(s)$  and between  $\mathbf{U}(s)$  and  $\mathbf{d}_1(s)$

$$\frac{\mathbf{y}}{\mathbf{d}_1}(s) = \frac{\mathbf{H}(s)}{1 + \mathbf{P}(s)\mathbf{C}(s)} \quad (78)$$

$$\frac{\mathbf{U}}{\mathbf{d}_1}(s) = \frac{-\mathbf{C}(s)\mathbf{H}(s)}{1 + \mathbf{P}(s)\mathbf{C}(s)} \quad (79)$$

where  $\mathbf{H}$  is defined by (53).

#### V. RESPONSE CURVES AND SIMULATIONS RESULTS

In this section, we consider the problem (1)-(4) where the coefficients are set to the following values

$$\lambda = \mu = 1, \quad \sigma^{+-} = 0.2, \quad \sigma^{-+} = 0.4, \quad q = 1, \quad \rho = 0.5$$

The numerical values of the parameters of this example are chosen such that the system is unstable [4]. Since the product  $|\rho q|$  is less than 1, one can arbitrarily choose the term  $\epsilon$  between 0 and 1 (see equation (28)). The goal of this section is to analyze deeper the role of the proposed degree of freedom and particularly the underlying trade-off.

##### A. Frequency response: Bode analysis

1) *Noise sensitivity function:* We compute for different values of  $\epsilon$  the Bode's gain of the noise sensitivity function. For this purpose the transfer functions are evaluated along the imaginary axis  $s = j\omega$ .

Figure 3 shows the gain of the noise sensitivity function

$$\mathbf{CS} = \frac{\mathbf{C}(j\omega)}{1 + \mathbf{P}(j\omega)\mathbf{C}(j\omega)}. \quad (80)$$

One can notice that the smaller  $\epsilon$  is, the lower the peaks of the Bode's gain are. This would mean that to reduce the

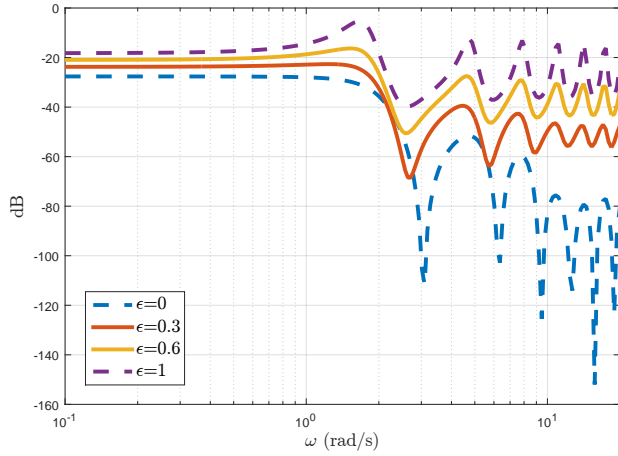


Fig. 4. Observer-controller,  $C$ , transfer function for different values of  $\epsilon$

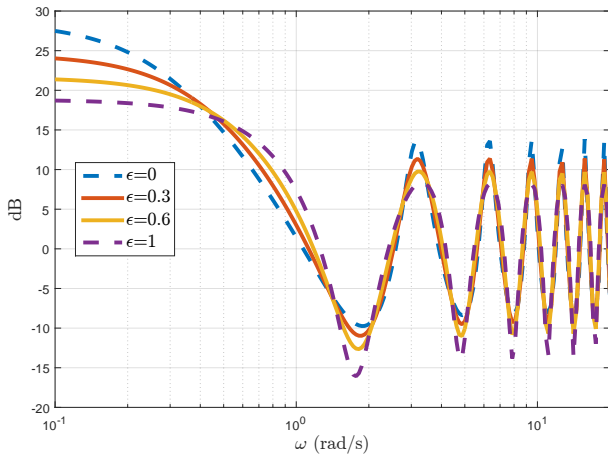


Fig. 5. Load sensitivity function for different values of  $\epsilon$

impact of the noise one should choose a small  $\epsilon$ . This is coherent since reducing  $\epsilon$  corresponds feeding in less of the measurement at the right boundary, c.f. (15). This is directly related to the fact that the control effort is smaller for a small  $\epsilon$  as shown in Figure 4, which shows the transfer function of  $C$  for different values of  $\epsilon$ .

2) *Load sensitivity function*: Figure 5 shows the gain of the load sensitivity function,  $\mathbf{PS}$ , where

$$\mathbf{PS}(j\omega) = \frac{\mathbf{P}(j\omega)}{1 - \mathbf{P}(j\omega)\mathbf{S}(j\omega)} \quad (81)$$

The results here seem to indicate that if the pulsation  $\omega$  is large enough, then the value of  $\epsilon$  does not play a preponderant role for the response of the system. However, for low to medium frequency ranges  $\omega < 0.4 \text{ rad/s}$ , it is clear that a larger value of  $\epsilon$  yields better performance in terms of rejection of transient disturbances in this frequency range. This result may however be treated carefully: for different system parameters (in particular with a higher  $\rho$ ) there can be a large variation between the response curves depending on the chosen value of  $\epsilon$ .

## B. Temporal response

To illustrate the previous result we simulate in Figs. 6–8 the response to a single square wave at the second disturbance input:  $d_2 = H(t) - H(t-1)$ , where  $H(\cdot)$  is the Heaviside step function. The Figures show the output  $y$  for different  $\epsilon$  with no noise (Fig. 6), and with noise (Fig. 7), and the control action  $u$  (Fig. 8).

Considering Fig. 6, it is clear that taking  $\epsilon = 1$  leads to a better response: the higher  $\epsilon$  is, the faster the convergence will be. With the addition of significant measurement noise, however, the results are more nuanced, see Fig. 7. Although the fast convergence rate is retained for  $\epsilon = 1$ , the high-frequency gain from the measurement to the actuation is much higher, causing significant deterioration of the performance and excessive use of the control action, see Fig. 8. Reducing the  $\epsilon$  reduces the effect of the noise on the system output  $y$  and the control action  $u$ , where for the extreme case  $\epsilon = 0$  the effect of the white noise is barely noticeable. These simulations clearly illustrate the trade-off between convergence rate and noise sensitivity made available by introduction of the  $\epsilon$  parameter.

## VI. CONCLUSION

Using the backstepping approach we have derived an extension to the observer presented in [17] in presence of disturbances in the system and of noise in the measurements. Nevertheless some aspects are neglected by such an approach since the trade-off between disturbance error reduction and sensor noise error reduction is not the only constraint on feedback design. For instance a lower value of  $\epsilon$  means a slower convergence to the equilibrium (in particular if there is no noise and if either  $\lambda$  or  $\mu$  is large). Moreover, the proposed approach does not reflect the influence of  $\epsilon$  on the size of the observer gains, shadowing the robustness aspects of the problem. Analyzing the impact of adding an integrator on the control law, as proposed in [13], to improve disturbance rejection will be the purpose of further contributions. Further, a similar degree of freedom can be added to the dual control design. Investigating such an addition, and extending to the case of multiple inputs will lead to compare the backstepping approach with the optimal control approaches derived in [12], [14] which lead to similar closed loop behavior.

## ACKNOWLEDGMENT

The work of the second author was supported by the Research Council of Norway, ConocoPhillips, Det norske oljeselskap, Lundin, Statoil and Wintershall through the research center DrillWell (203525/O30) at IRIS.

## REFERENCES

- [1] Saurabh Amin, Falk M Hante, and Alexandre M Bayen. On stability of switched linear hyperbolic conservation laws with reflecting boundaries. In *Hybrid Systems: Computation and Control*, pages 602–605. Springer, 2008.
- [2] Karl Johan Åström and Richard M. Murray. *Feedback systems: an introduction for scientists and engineers*. Princeton university press, 2nd edition, 2010.

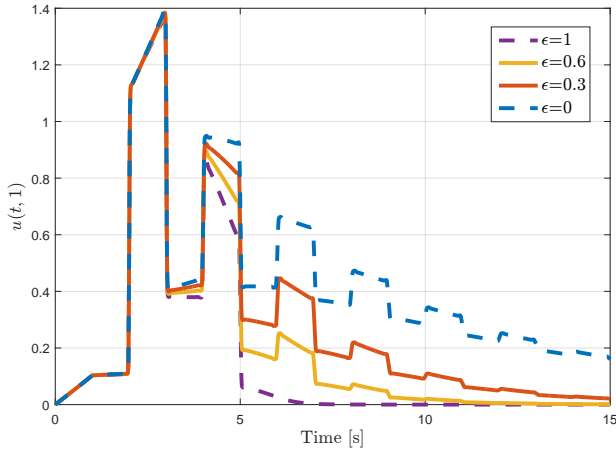


Fig. 6. Response to a single (amplitude and period of one) square wave disturbance at  $d_2$  for different values of  $\epsilon$ .

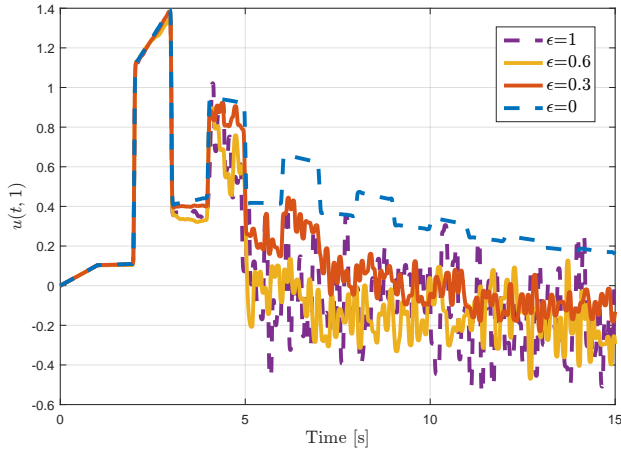


Fig. 7. Response to a single (amplitude and period of one) square wave disturbance at  $d_2$  for different values of  $\epsilon$  with white noise at  $n$ .

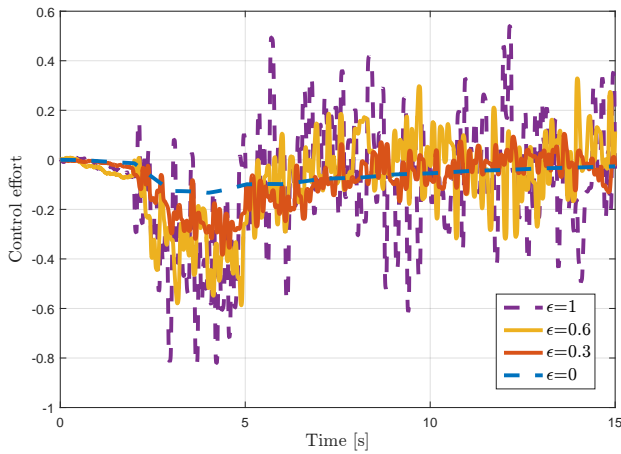


Fig. 8. Control effort response to a single (amplitude and period of one) square wave disturbance at  $d_2$  for different values of  $\epsilon$ .

- [3] Jean Auriol and Florent Di Meglio. Minimum time control of heterodirectional linear coupled hyperbolic pdes. *Automatica*, 71:300–307, 2016.
- [4] G Bastin and JM Coron. Stability and boundary stabilization of 1-d hyperbolic systems. *Preprint*, 2015.
- [5] Jean-Michel Coron, Brigitte Andréa-Novel, and Georges Bastin. A lyapunov approach to control irrigation canals modeled by saint-venant equations. In *Proc. European Control Conference, Karlsruhe*, 1999.
- [6] Jean-Michel Coron, Rafael Vazquez, Miroslav Krstic, and Georges Bastin. Local exponential  $h^2$  stabilization of a  $2 \times 2$  quasilinear hyperbolic system using backstepping. *SIAM Journal on Control and Optimization*, 51(3):2005–2035, 2013.
- [7] Ruth Curtain and Kirsten Morris. Transfer functions of distributed parameter systems: A tutorial. *Automatica*, 45(5):1101–1116, may 2009.
- [8] Jonathan de Halleux, Christophe Prieur, J-M Coron, Brigitte d’Andréa Novel, and Georges Bastin. Boundary feedback control in networks of open channels. *Automatica*, 39(8):1365–1376, 2003.
- [9] Florent Di Meglio. *Dynamics and control of slugging in oil production*. PhD thesis, École Nationale Supérieure des Mines de Paris, 2011.
- [10] Stéphane Dudret, Karine Beauchard, Fouad Ammouri, and Pierre Rouchon. Stability and asymptotic observers of binary distillation processes described by nonlinear convection/diffusion models. In *American Control Conference (ACC), 2012*, pages 3352–3358. IEEE, 2012.
- [11] Long Hu, Florent Di Meglio, Rafael Vazquez, and Miroslav Krstic. Control of homodirectional and general heterodirectional linear coupled hyperbolic pdes. *IEEE Transactions on Automatic Control*, 61(11):3301–3314, 2016.
- [12] H. L. Koh. *Structure of Riccati Equation Solutions in Optimal Boundary Control of Hyperbolic Equations with Quadratic Cost Functionals*. PhD thesis, 1976.
- [13] Pierre-Olivier Lamare and Florent Di Meglio. Adding an integrator to backstepping: Output disturbances rejection for linear hyperbolic systems. In *American Control Conference (ACC), 2016*, pages 3422–3428. IEEE, 2016.
- [14] D. L. Russell. Controllability and stabilizability theory for linear partial differential equations: recent progress and open questions. *Siam Review*, 20(4):639–739, 1978.
- [15] Rafael Vazquez, Jean-Michel Coron, Miroslav Krstic, and Georges Bastin. Local exponential  $h^2$  stabilization of a  $2 \times 2$  quasilinear hyperbolic system using backstepping. In *Decision and Control and European Control Conference (CDC-ECC), 2011 50th IEEE Conference on*, pages 1329–1334. IEEE, 2011.
- [16] Rafael Vazquez and Miroslav Krstic. Marcum q-functions and explicit kernels for stabilization of  $2 \times 2$  linear hyperbolic systems with constant coefficients. *Systems & Control Letters*, 68:33–42, 2014.
- [17] Rafael Vazquez, Miroslav Krstic, and Jean-Michel Coron. Backstepping boundary stabilization and state estimation of a  $2 \times 2$  linear hyperbolic system. *IEEE Conference on Decision and Control and European Control Conference*, 1(1):4937–4942, dec 2011.
- [18] Rafael Vazquez, Miroslav Krstic, and Jean-Michel Coron. Backstepping boundary stabilization and state estimation of a  $2 \times 2$  linear hyperbolic system. In *Decision and Control and European Control Conference (CDC-ECC), 2011 50th IEEE Conference on*, pages 4937–4942. IEEE, 2011.
- [19] Cheng-Zhong Xu and Gauthier Sallet. Exponential stability and transfer functions of processes governed by symmetric hyperbolic systems. *ESAIM: Control, Optimisation and Calculus of Variations*, 7:421–442, 2002.
- [20] Kemin Zhou, John Comstock Doyle, Keith Glover, et al. *Robust and optimal control*, volume 40. Prentice hall New Jersey, 1996.